Tube Array Heat Transfer in Fluidized Beds A Study of Particle Size Effects

Experiments were performed with an array of horizontal tubes, arranged in a regular equilateral triangular pattern, immersed in a fluidized bed operating at 812 K. Data are reported for heat transfer between the bed and a centrally-located tube in the array. Both total and radiative heat transfer rates were measured for superficial velocities spanning the range from packed bed conditions to over twice the minimum fluidization velocity. Results are presented for five different-size particles. Local heat transfer values, measured around the tube periphery, and integrated averages are reported for all test conditions.

Comparisons are also made between the heat transfer behavior of a tube in an array and that for a single tube in a hot fluidized bed under the same overall operating conditions. The results of this comparison suggest that the two mechanisms, gas convection and radiation, are competing effects.

Tae-Yong Chung
James R. Welty
Department of Mechanical Engineering
Oregon State University
Corvallis, OR 97331

Introduction

The use of fluidized beds of large particles as combustion zones for coal-fired power plants has generated interest in the heat transfer capabilities of these devices. The ability of limestone to adsorb SO_x makes fluidized beds composed of limestone particles attractive from the standpoint of rendering airborne emissions more environmentally acceptable. It happens that the dynamic character of fluidized beds also enhances heat transfer rates between hot beds and immersed surfaces which, in the power plant application, would be arrays of tubes carrying the water-steam working fluid. Improved heat transfer characteristics allow the desired energy transport to occur at lower-than-normal temperatures, thereby decreasing NO_x emissions also.

These attractive devices involve fluid behavior that is so chaotic that an analysis of the heat transfer process, from first principles, is presently out of the question. Numerical simulations of varying degrees of complexity have achieved limited success; all must be compared with experimental measurements for validation.

One facet of high temperature operation, at conditions representative of actual combustion processes, is the contribution of radiation to total energy transport. The experimental facility at Oregon State University, which was used in the work described in this paper, is one of very few with the capability of high temperature operation, with proven instrumentation capable of simultaneous determination of both total and radiant heat transfer rates.

The experimental results reported herein are among the first that relate local total and radiant heat transfer coefficients, in a tubular array geometry, as affected by bed particle size and bed superficial velocity at temperatures representative of combustion operation. Most data reported previously were acquired at low temperatures, thus radiant contributions were either ignored or inferred.

The data acquired in this study are presented as plots of both total and radiative heat transfer coefficients as functions of bed operating parameters, all at a bed temperature of 812 K.

Characteristic heat transfer behavior is demonstrated, as heat transfer rates increase from the packed-bed state through minimum fluidization and through a range in superficial velocities greater than twice the minimum fluidization values. Heat transfer rates were always the greatest for the smaller particles tested at all test conditions. The effects of bubble motion, characteristic of higher superficial velocities, in displacing the stagnant particle cap from the top of the tubes is apparent.

A dimensionless representation of maximum Nusselt number as a function of Archimedes number shows reasonable agreement with the generally-accepted correlations using these parameters.

Current address of T.-Y. Chung: Department of Medical Engineering, Kookmin University, Seoul, 132, Korea.

Relevance of the Present Work

Gas-solid fluidized bed combustors are noted for their excellent heat transfer characteristics; it is generally acknowledged that high rates of heat transfer can be achieved between the bed and immersed surfaces or vessel walls. A fundamental knowledge of heat transfer in high-temperature fluidized beds is essential for proper design and optimization of such a combustor. High-temperature heat transfer is significantly difficult to describe since the convective and radiative heat transfer occur simultaneously. Fluidized-bed heat transfer phenomena are complicated further due to the large number of important bed parameters which affect transport, among those parameters of importance are: bed and heat transfer surface temperatures; particle size, shape and physical properties; type of distributor; fluidizing velocity; and configuration of the immersed surfaces such as size, shape, spacing and pitch.

A large number of investigations (Alavizadeh, 1985; Goshayeshi et al., 1985; Lei, 1988; Mathur and Saxena, 1987), reported in the literature, have emphasized spatial-averaged heat transfer results. Local, time-averaged heat transfer coefficients for an immersed tube array provide additional information of importance to the fluidized-bed combustor designer. A number of recent investigations have reported local heat transfer results. Most of the previous investigations were restricted to small particles, a single tube, and low bed temperatures where tubes were electrically heated and local heat fluxes were evaluated by measuring the power input, along with measurements of tube wall temperatures, for heat transfer coefficient calculations (Goshayeshi et al., 1985).

The objective of the present work is to measure the local bed-to-tube total and radiative heat transfer rates for a horizontal tube array immersed in a high-temperature fluidized bed. A well-designed instrumented tube capable of measuring both total and radiative heat transfer coefficients between the bed and immersed surfaces, developed by Alavizadeh et al. (1984) and Lei (1988), was employed to evaluate the effect of different bed parameters.

Experimental Apparatus

Figure 1 illustrates an instrumented tube capable of measuring both the total and radiative heat transfer coefficients between the bed and immersed tubes. The instrumented tube, with outside and inside diameters of 51 mm and 32 mm, was made of bronze and equipped with three total and three radiative heat transfer measuring devices. They were mounted side-by-side, each 90 degrees apart, along the axis of the tube.

The microfoil thermopile-type heat flow detector formed by a thin, low-thermal-conductivity film with a thermopile on each side was employed as a total and radiative heat flux sensor. Total heat flux sensors were bonded to the tube surface with epoxy and then covered by the 0.127-mm-thick stainless steel shim to protect them from bed abrasion. The shim was pulled tightly over the sensors and connected to the tube with a clamp. A thin film of high-conductivity compound was deposited between the sensors and the shim to reduce thermal contact resistance. Radiation detectors, originally developed by Alavizadeh et al. (1984) and modified by Lei (1988), were used in this work. The radiative component of the total heat transfer from the bed was transmitted through a transparent window mounted on the top of a cavity within the instrumented tube and

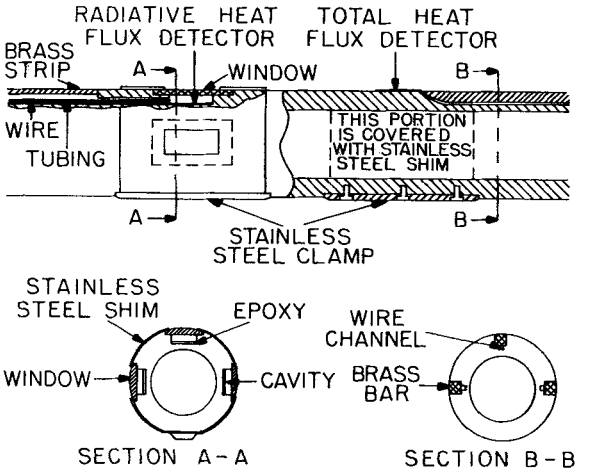

Figure 1. Instrumented tube for total and radiative heat flux measurements.

detected by a heat flux sensor bonded to the base of the cavity. Silicon was employed as the window material and was machined to have the same curvature as the outside of the tube. Silicon has been found to be the superior window material among silicon, sapphire, crystal quartz and fused quartz as potential candidates for the transmitting window medium (Alavizadeh et al., 1984).

Figure 2 shows the experimental equipment. Measurements were conducted in the Oregon State University high-temperature fluidized-bed facility.

Combustion air was compressed and introduced into the system using an air blower. Propane was fed into the burner and burned in a refractory-lined combustion chamber. The hot combustion gases were directed into the 0.3 × 0.6 m test section through an inconel distributor plate. No combustion occurred in the fluidized bed itself. A proportional-type controller was used to regulate the propane flow rate and maintain the desired gas temperature.

An array of nine bronze tubes, each with an outside diameter of 51 mm, arranged in three horizontal rows, was used. This staggered arrangement, shown in Figure 3, is among the most common in-bed tube designs in industrial fluidized-bed combustors (Alavizadeh et al., 1984; Strom et al., 1977; Welty, 1983). The instrumented tube was placed in the center of the nine tubes to represent typical conditions of a tube in an actual large-bed array. The tubes were cooled by circulating water. A rotary union was used to adjust the instrumented tube to desired angular positions for data collection.

A high-precision digital data acquisition system (HP-3497A) with an HP-85 microcomputer connected with an HP-IB interface card and a dual disk drive (HP-83901M) as a control unit was used to record local heat fluxes and surface temperatures and compute local heat transfer coefficients at each position on the instrumented tube.

Experiments

Experiments were conducted at a bed temperature of 812 K. A granular refractory (Ione grain) was used as bed material with mean particle diameters of 0.97, 1.53 and 2.37 mm. The mean particle diameter was calculated from the equation sug-

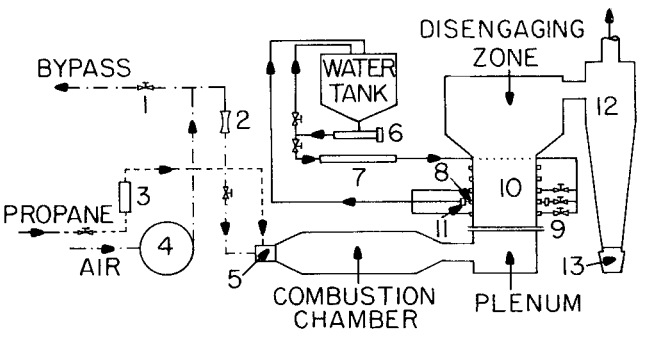

Figure 2. Experimental facility.

gested by Kunii and Levenspiel (1969). Table 1 show particle size distribution, chemical composition as given by the supplier and properties (Ghafourian, 1984) of Ione grain.

Data were taken at 0, 45, 90, 135 and 180 degrees from the lower stagnation point. Calibration of the heat flux sensor was performed, prior to delivery, by the manufacturer. The calibration to relate the heat flux detected by the sensor to the actual radiation absorbed by the tube wall was carried out locally using a narrow-angle black body source. Details of the calibration techniques and procedures can be found in Alavizadeh (1985) and Alavizadeh et al. (1984).

Results and Discussion

All radiative heat transfer coefficients and the radiation contribution in percentage of the total, reported in this study, were calculated for a black tube wall. The values of local total heat transfer coefficient reported in this study are within the range (+0.08, −0.14) of actual values, and those of local radiative heat transfer coefficient are within the range (+0.125, −0.115) of actual values. Values shown for mean particle diameters of 2.14 and 3.23 mm are data acquired by Lei (1988).

Figures 4 and 5 shows results of the spatial-averaged total and radiative heat transfer coefficients, respectively, for different particle sizes as functions of superficial velocity for a bed temperature of 812 K. As the superficial velocity approached the minimum fluidizing velocity (U_{mf}), the spatial-averaged total and radiative heat transfer coefficients increased sharply due to the induced particle motion causing replacement of cold particles near the tube wall. The spatial-averaged total heat transfer coefficients increased gradually, reaching maximum values at superficial velocities somewhat greater than the minimum fluidizing velocity, then decreased slowly in all cases. This decrease can be attributed to a decrease in bed density and greater bubble contract fraction accompanying the increase in superficial velocity. As superficial velocity increased beyond U_{mf}, spatial-averaged radiative heat transfer coefficients increased very gradually, and appear to be approaching an asymptotic value. Similar trends have been observed by other investi-

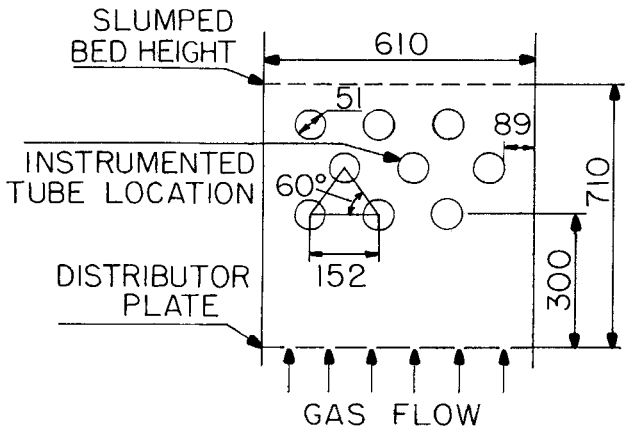

Figure 3. Tube array geometry.

Table 1. Size Distribution, Composition and Properties of the Particles

Mesh No.	D_{pi} (mm)	Mass Fraction (%) Sample A	Sample B	Sample C
5–6	3.675	*	*	5.25
6–8	2.855	*	11.19	44.25
8–10	2.180	*	25.36	28.32
10–12	1.850	*	19.11	20.06
12–14	1.550	7.40	9.99	2.22
14–16	1.290	14.72	9.34	*
16–20	1.015	54.27	21.97	*
20–30	0.725	21.20	3.04	*
30–40	0.513	2.41	*	*
Mean Particle Size, $\overline{D}_p$(mm)		0.97	1.53	2.37
Standard Deviation (mm)		0.398	1.035	0.878

Chemical Composition: Silica, 53.5%; Alumina, 43.8%; Titania, 2.3%; Others, 0.4%

Properties

ρ_p = 2,700 kg/m^3

C_{ps} = 0.853 − 0.982 kJ/kg · K (470–900 K)

k_p = 1.1 − 1.41 W/m · K (494–833 K)

ϵ_p = 0.855 − 0.874 (279–452 K)

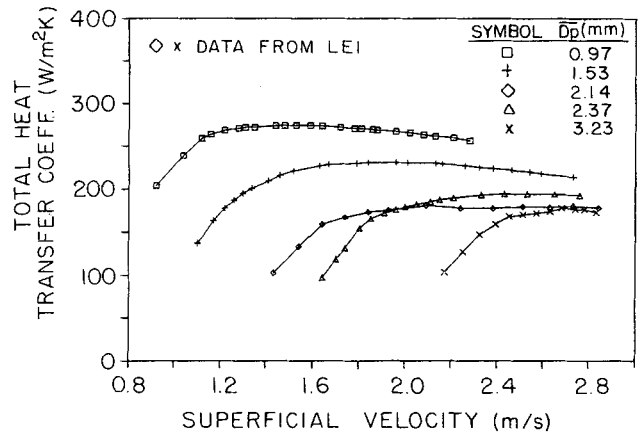

Figure 4. Total heat transfer coefficients (spatially-averaged) as functions of particle size and superficial velocity.

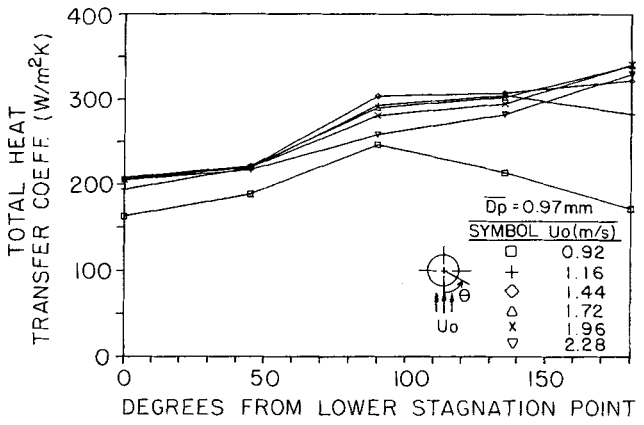

Figure 6. Variation of local total heat transfer coefficient with superficial velocity: mean particle diameter = 0.97 mm.

gators (Alavizadeh, 1985; Alavizadeh et al., 1984; Vadivel and Vedamurthy, 1980).

Figures 6, 7 and 8 show time-averaged local total heat transfer coefficients for mean particle diameters of 0.97, 1.53 and 2.37 mm, respectively. These figures illustrate the time-averaged local total heat transfer coefficient around the surface of the tube for six superficial velocities. One value of velocity is below U_{mf}; the others are in the fluidization range. The most obvious effect is the very large change in magnitude of the local total heat transfer coefficient at the upper stagnation point as the superficial velocity was increased. At the lower stagnation point, values of the local total heat transfer coefficient increased with superficial velocity until U_{mf} was reached. Values were insensitive to additional changes above the minimum fluidizing velocity.

In Figure 6, values of local total heat transfer coefficients at the upper stagnation point were observed to increase from 172 to 342 W/m² · K for increases in superficial velocity from 0.92 to 2.28 m/s. At the lower stagnation point, these values increased from 163 to 208 W/m² · K over the same range of superficial velocity. Above U_{mf}, values at this location remained in a narrow range between 194 and 200 W/m² · K.

Values of the time-averaged local radiative heat transfer coefficients for a representative tube in an array are displayed in Figures 9, 10 and 11. Each figure shows results for the same condition as in Figures 6, 7 and 8, respectively. They demonstrate similar tendencies for all particle sizes. Values of local radiative heat transfer coefficients are relatively low for a packed-bed condition. Local radiative heat transfer coefficients at all locations increased with superficial velocity, the ratio of increase with U_o increasing directly as the distance from the lower stagnation point for all operating conditions. More uniform distributions of local radiative heat transfer coefficients were established for higher values of superficial velocity.

In the case with a mean particle diameter of 2.37 mm, values of the local radiative heat transfer coefficient at the upper stagnation point increased from 1 to 21 W/m² · K for values of superficial velocity varying from 1.64 to 2.76 m/s; at the lower stagnation point increases between 17 and 23 W/m² · K were measured over this same superficial velocity range.

The relatively low values for local coefficients on the upper half of the tube at low superficial velocities are due to the presence of the relatively cool stagnant defluidized particle cap, the so-called "lee stack." However, at velocities above minimum fluidization, the cap was displaced by rising bubbles. Values of

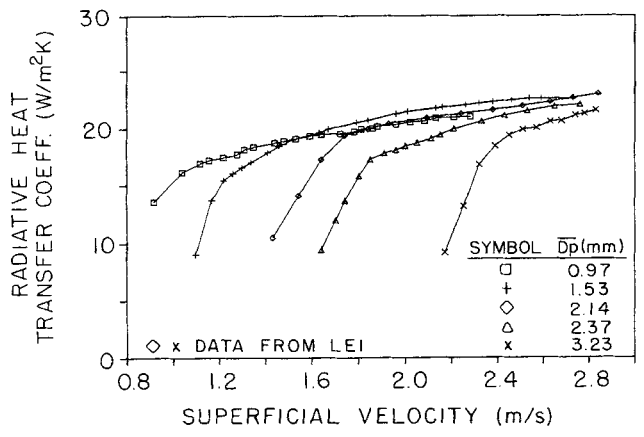

Figure 5. Radiative heat transfer coefficients (spatially-averaged) as functions of particle size and superficial velocity.

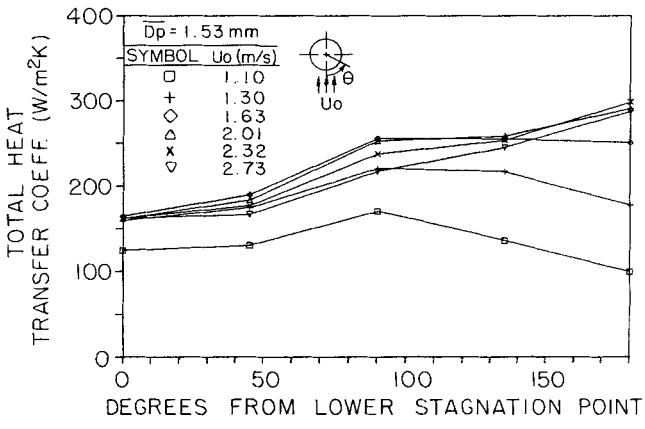

Figure 7. Variation of local total heat transfer coefficient with superficial velocity: mean particle diameter = 1.53 mm.

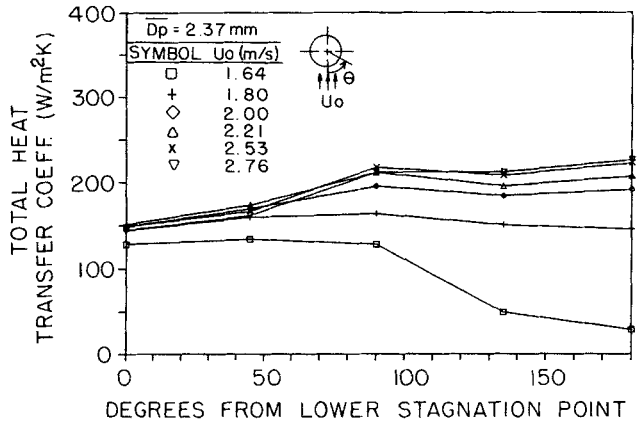

Figure 8. Variation of local total heat transfer coefficient with superficial velocity: mean particle diameter = 2.37 mm.

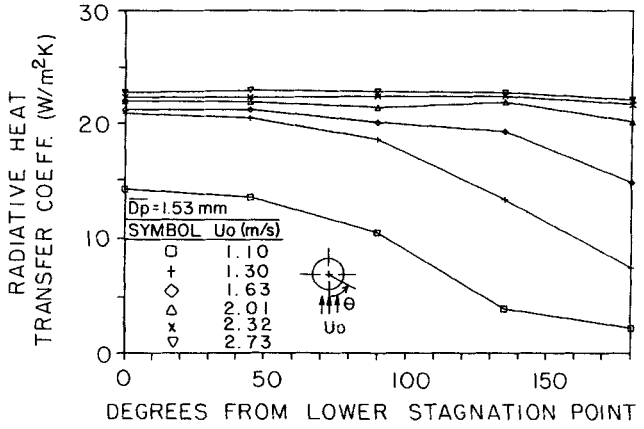

Figure 10. Variation of local radiative heat transfer coefficient with superficial velocity: mean particle diameter = 1.53 mm.

local heat transfer coefficients over the lower part of the tube were relatively insensitive to changes in superficial velocity as a result of a gas layer surrounding the lower portion of the tube (Hager and Thomson, 1973; Rowe, 1976).

Figure 12 shows values for the spatial-averaged maximum total heat transfer coefficient and the radiation contribution at the same conditions as functions of the mean particle diameter, for a bed operating temperature of 812 K. Values of the maximum spatial-averaged heat transfer coefficients decreased from 275 to 178 $W/m^2 \cdot K$ for mean particle diameters increasing from 0.97 to 3.23 mm. Radiation contributions increased with an increase in mean particle size. Even though the radiant contribution was observed to increase with particle size, the observed decrease in maximum heat transfer coefficients with an increase in particle size is in agreement with generally-accepted fluidized bed behavior.

Figures 13 and 14 show comparisons of time-averaged local total and radiative heat transfer coefficients, respectively, for the condition of maximum total heat transfer at a bed temperature of 812 K. With the spatial-averaged total heat transfer coefficient maintained at its maximum value, the required superficial velocity was greater for larger mean particle sizes. Values of local total heat transfer coefficients on the lower half of the tube were found to be lower than those on the upper half for the smaller particles. For larger particle sizes, values of the local total heat transfer coefficient around the tube appear almost uniform. Values of local radiative heat transfer coefficients at maximum total heat transfer conditions tend to decrease slightly with distance from the lower stagnation point.

Figure 15 shows the relationship between the maximum Nusselt number and Archimedes number for the present work along with results of other studies, Lei (1988) and Goshayeshi et al. (1985), all for a tube in an array. Nusselt numbers and Archimedes numbers were calculated using air properties at operating bed temperatures. Data for the present work agree closely with Baskakov's correlation (Baskakov et al., 1973 a,b), shown in the figure as a solid line.

Comparison with Single-Tube Performance

Evaluating the heat transfer performance of a tube in an array is a practical yet difficult task. Entirely different test sections must be fabricated if one is to vary tube size, arrangement, or spacing. It is, obviously, much easier to study single tubes, however, depending upon an array configuration, bed hydrodynamics could be very different with a direct influence on heat

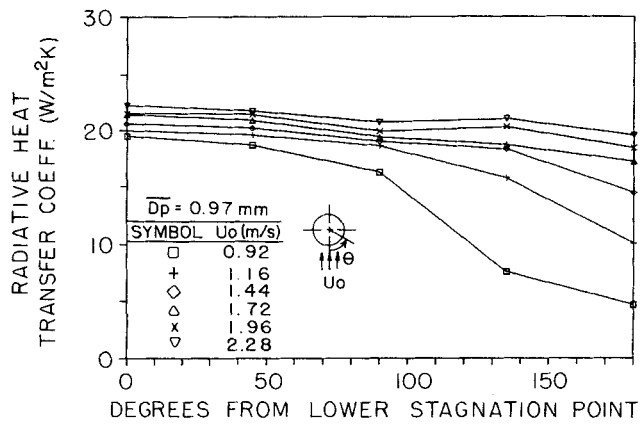

Figure 9. Variation of local radiative heat transfer coefficient with superficial velocity: mean particle diameter = 0.97 mm.

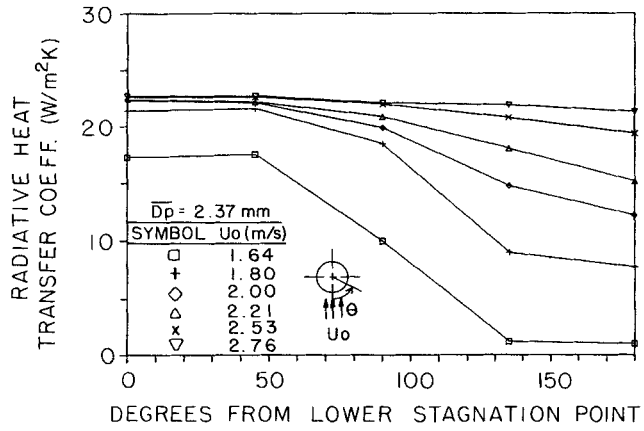

Figure 11. Variation of local radiative heat transfer coefficient with superficial velocity: mean particle diameter = 2.37 mm.

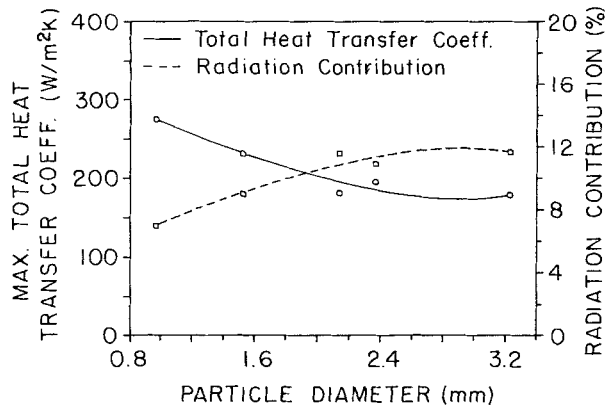

Figure 12. Maximum total and radiative heat transfer (spatially-averaged) as functions of mean particle diameter.

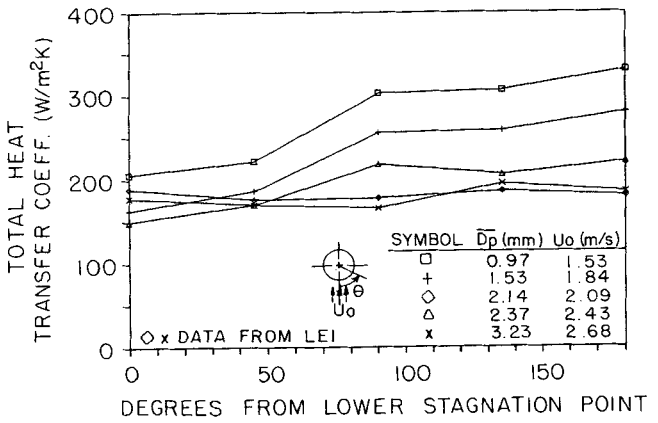

Figure 13. Variation of local total heat transfer coefficients at conditions of maximum total heat transfer.

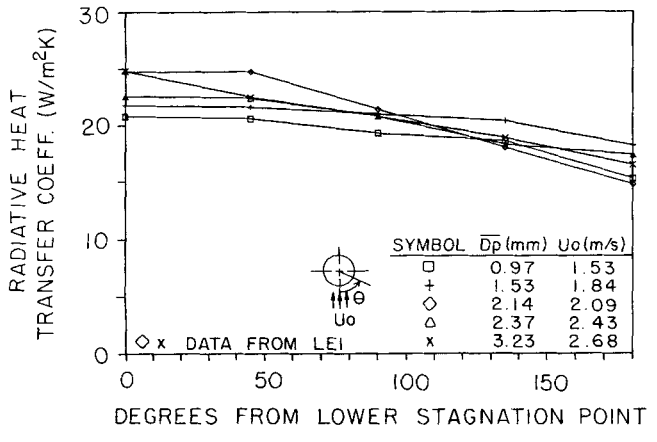

Figure 14. Variation of local radiative heat transfer coefficient at conditions of maximum total heat transfer.

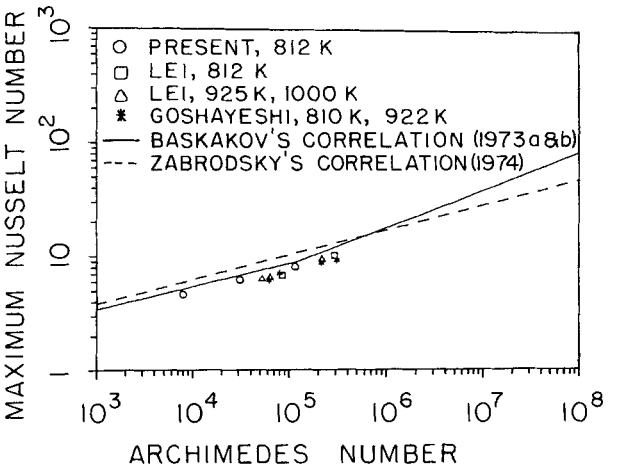

Figure 15. Maximum Nusselt number variation with Archimedes number.

transfer behavior. This holds true for both particle and gas convection–processes which are directly coupled with fluid mechanical behavior.

Radiation effects are also dependent on array geometry. It is possible, for example, in a vigorously bubbling bed with close tube spacings, for a tube to have a direct view of one or more neighboring tubes. This would obviously not be true in the case of a single tube.

Figures 16 and 17 compared heat transfer coefficients, both total and radiative, for a tube in an array and for a tube by itself. The single-tube data have been previously reported by Alavizadeh et al. (1985); they were obtained using the same apparatus and for the same operating conditions as in the present work.

Values of the total heat transfer coefficient are compared in Figure 16. For the case of $U/U_{mf} < 1$ the single tube exhibits larger values of h and the condition of minimum fluidization can be seen with some definition. The case of a tube in an array is seen to follow the same general trends as for a single tube, however minimum fluidization is less distinct and appears to occur at a higher superficial velocity. When both tubes are in the fluidized regime the heat transfer coefficients have approximately the same values. There is some indication that the array values

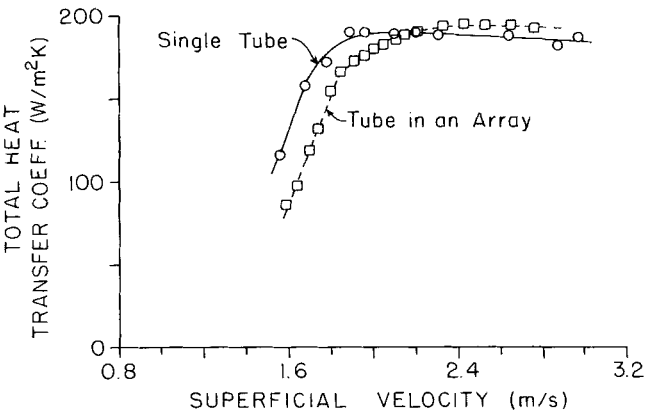

Figure 16. Total heat transfer: array vs. single-tube performance.

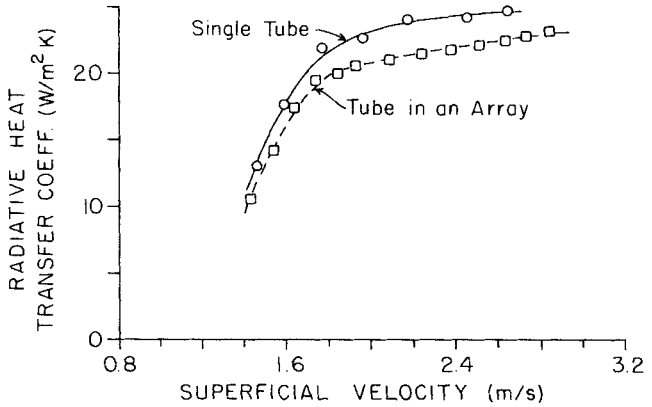

Figure 17. Radiative component: array vs. single-tube performance.

are a bit higher, but by no more than 5% over the velocity range examined. The influence of near tubes tends to reduce the tendency of the stack to exist for long, if at all, thus the convective component in the case of an array would be expected to be larger.

A comparison of the radiant contributions is shown in Figure 17. It is clear that a single tube will receive more heat by radiation than for one in an array, and for all velocities. The difference is greater in the fluidization regime. The effective bed temperature for radiant transfer to a tube in an array would certainly be lower than for a single tube, thus the decrease in h_{radiant} for the array case is as expected. Since these quantitative results are specific for the array geometry of this work, we do not suggest a specific value for the differences in total and radiant heat transfer coefficients between the two cases. Qualitatively these results are valid. The differences should decrease as the spacing between adjacent tubes in an array is increased.

A final comment regarding this comparison relates to the competing heat transfer mechanisms of gas convection and radiation. Since the contribution of convection to total heat transfer is increased when a tube has near neighbors, and that of radiation is decreased, an absolute comparison between the behavior of a tube in an array with a single tube will depend on which of the two effects is the larger. For the present case—at the temperature, particle size, and array geometry used for comparison—the two competing effects almost cancel with some evidence of enhanced convection being the larger influence at velocities in the bubbling-bed regime.

Acknowledgment

Appreciation is expressed to Korea Science and Engineering Foundation (KOSEF) whose support provided the means for the first author (T. Y. Chung) to spend the necessary time in the United States for this work to be accomplished.

Notation

Ar = Archimedes number = $g\bar{D}_p^3[\rho_p - \rho_f]/\mu_f^2$
C_{ps} = particle specific heat at constant pressure
D_p = particle diameter
$\bar{D}_p$ = mean particle diameter
$\bar{D}_{pi}$ = mean open diameter in sieve
g = gravitational acceleration
$\bar{h}_{\max}$ = spatial-averaged maximum total heat transfer coefficient
k_f = gas thermal conductivity
k_p = particle thermal conductivity
$\overline{Nu}_{\max}$ = spatial-averaged maximum Nusselt number = $\bar{h}_{\max}\bar{D}_p/k_f$
U_{mf} = minimum fluidizing velocity
U_o = superficial velocity
ρ_f = gas density
ρ_p = particle density
μ_f = gas viscosity
ϵ_p = particle emissivity
θ = angle from lower stagnation point, degrees

Literature Cited

Alavizadeh, N., "An Experimental Investigation of Radiative and Total Heat Transfer Around a Horizontal Tube," PhD. Thesis, Dept. of Mech. Eng., Oregon State Univ. (Aug., 1985).

Alavizadeh, N., R. L. Adams, J. R. Welty, and A. Goshayeshi, "An Instrument for Local Radiative Heat Transfer Measurement in a Gas Fluidized Bed at Elevated Temperature," *New Experimental Techniques in Heat Transfer,* Nat. Heat Transfer Conf. and Exhibition, ASME HTD, **31,** 1 (1984).

Alavizadeh, N., Z. Fu, R. L. Adams, J. R. Welty, and A. Goshayeshi, "Radiative Heat Transfer Measurement for a Horizontal Tube Immersed in Small and Large Particle Fluidized Beds," Int. Symp. in Heat Transfer, Beijing, China (Oct., 1985).

Baskakov, A. P., B. V. Berg, O. K. Vitt, N. F. Filippovsky, V. A. Kirakosyan, J.M. Goldobin, and V. K. Maskaev, "Heat Transfer to Objects Immersed in Fluidized-Beds," *Power Technol.,* No. 8, 273 (1973).

Baskadov, A. P., O. K. Vitt, V. A. Kirakosyan, V. K. Maskaev, and N. F. Filippovsky, "Investigation of Heat Transfer Coefficient Pulsations and of the Mechanism of Heat Transfer from a Surface Immersed into a Fluidized Bed," *La Fluidisation et Ses Applications-Congress International,* **1,** Cepadues, Toulouse, France (Oct., 1973).

Ghafourian, N. R., "Determination of Thermal Conductivity, Specific Heat and Emissivity of Ione Grain," MS Project, Dept. of Mech. Eng., Oregon State Univ. (June, 1984).

Goshayeshi, A., J. R. Welty, R. L. Adams, and N. Alavizadeh, "Local Heat Transfer Coefficients for Horizontal Tube Arrays in High Temperature Large Particle Fluidized Beds—An Experimental Study," *AIChE Symp. Ser.,* **81**(245), (1985).

Hager, W. R., and S. D. Schrag, "Particle Circulation Downstream from a Tube Immersed in a Fluidized Bed," *Chem. Eng. Sci.,* **31,** 657 (1976).

Hager, W. R., and W. J. Thomson, "Bubble Behavior around Immersed Tubes in a Fluidized Bed," *AIChE, Symp. Ser.,* **69** (128), (1973).

Kunii, D., and O. Levenspiel, *Fluidization Engineering,* Wiley (1969).

Lei, D. H., "An Experimental Study of Radiative and Total Heat Transfer between a High Temperature Fluidized Bed and an Array of Immersed Tubes," PhD. Thesis, Dept. of Mech. Eng., Oregon State Univ. (Jan., 1988).

Mathur, A., and S. C. Saxena, "Total and Radiative Heat Transfer to an Immersed Surface in a Gas-Fluidized Bed," *AIChE J.,* **33** (7), 1124 (July, 1987).

Rowe, P. N., "Prediction of Bubble Size in a Gas Fluidized Bed," *Chem. Eng. Sci.,* **31,** 1081 (1976).

Strom, S. S., T. E. Dowdy, W. C. Lapple, J. B. Kitto, T. P. Stanoch, R. H. Boll, and W. L. Sage, "Preliminary Evaluation of Atmospheric Pressure Fluidized Bed Combustion Applied to Electric Utility Large Steam Generators," EPRI Report, No. RP 412-1, Electric Power Res. Inst., Palo Alto, CA (Feb., 1977).

Vadivel, R., and V. N. Vedamurthy, "An Investigation of the Influence of Bed Parameters on the Variation of the Local Radiative and Total Heat Transfer around an Embedded Horizontal Tube in a Fluidized Bed Combustor," *Proc. Int. Conf. on Fluidized Bed Combustion,* **3,** Atlanta (Apr., 1980).

Welty, J. R., "Heat Transfer in Large Particle Fluidized Beds," *U.S./CHINA Binational Heat Transfer Workshop,* Z. Wu, B. Wang, C. L. Tien, and K. T. Yang, eds., (Oct., 1983).

Zabrodsky, S. S., N. V. Antonishin, G. M. Vasiliev, and A. L. Paranas, "The Choice of Design Correlation for the Estimation of the High-Temperature Fluidized Bed-to-Immersed Body Heat Transfer Coefficient," *Vestn. Akad. Nauk. USSR,* Ser. Fiz-Energ. Nauk No. 4, 103 (1974).

Manuscript received June 27, 1988, and revision received Feb. 23, 1988.